

Research Article

Adaptive patient-cooperative compliant control of lower limb rehabilitation robot

Lingling Chen^{a,b,*}, Jiabao Huang^a, Yanglong Wang^a, Shijie Guo^{b,c}, Mengge Wang^d, Xin Guo^{a,b}^a School of Artificial Intelligence, Hebei University of Technology, Tianjin 300400, China^b Intelligent Rehabilitation Device and Detection Technology Engineering Research Centre of the Ministry of Education, Tianjin 300400, China^c School of Mechanical Engineering, Hebei University of Technology, Tianjin 300400, China^d School of Electrical Engineering, Hebei University of Technology, Tianjin 300400, China

ARTICLE INFO

Article history:

Received 29 December 2023

Revised 6 March 2024

Accepted 11 March 2024

Available online 16 March 2024

Keywords:

Compliant control

Lower limb rehabilitation robot (LLRR)

Adaptive admittance controller

Adaptive backstepping controller

Human-robot interaction

ABSTRACT

With the increase in the number of stroke patients, there is a growing demand for rehabilitation training. Robot-assisted training is expected to play a crucial role in meeting this demand. To ensure the safety and comfort of patients during rehabilitation training, it is important to have a patient-cooperative compliant control system for rehabilitation robots. In order to enhance the motion compliance of patients during rehabilitation training, a hierarchical adaptive patient-cooperative compliant control strategy that includes patient-passive exercise and patient-cooperative exercise is proposed. A low-level adaptive backstepping position controller is selected to ensure accurate tracking of the desired trajectory. At the high-level, an adaptive admittance controller is employed to plan the desired trajectory based on the interaction force between the patient and the robot. The results of the patient-robot cooperation experiment on a rehabilitation robot show a significant improvement in tracking trajectory, with a decrease of 76.45% in the dimensionless squared jerk (DSJ) and a decrease of 15.38% in the normalized root mean square deviation (NRMSD) when using the adaptive admittance controller. The proposed adaptive patient-cooperative control strategy effectively enhances the compliance of robot movements, thereby ensuring the safety and comfort of patients during rehabilitation training.

© 2024 The Author(s). Published by Elsevier B.V. on behalf of Shandong University. This is an open access article under the CC BY-NC-ND license (<http://creativecommons.org/licenses/by-nc-nd/4.0/>).

1. Introduction

With the increasing aging population, there has been a rise in the number of patients suffering from neurological and muscular diseases, which often result in long-term disability [1]. Physiotherapists provide physical therapy as a means to help these patients regain their motor function [2]. However, the growing number of stroke patients has posed a challenge to physical therapy as there is a limited number of physiotherapists available [3]. In recent decades, there has been a growing interest in incorporating robots into rehabilitation therapy [4–6]. Robot-assisted rehabilitation has the potential to address labor intensiveness and the lack of repeatability associated with manual therapy [7].

Currently, rehabilitation robots can be classified into two main types: exoskeleton and end effector. Exoskeleton rehabilitation devices enable coordinated movement training of multiple joints as well as independent movement training of single joints, having strong training pertinence. For instance, Peng et al. [8] developed

a wearable exoskeleton robot called the Funabot-Suit, which assists individuals in performing four basic movements: bending back and forth, as well as twisting left and right. On the other hand, the end effector type of rehabilitation robot offers several advantages, including a simpler structure, better human-robot compatibility, and the ability to adjust system stiffness. Dong et al. [9] designed an end-effector type lower limb rehabilitation robot called LOBO, which facilitates simultaneous and continuous rehabilitation training of the hip, knee, and ankle joints in space.

There are two common methods of training in robot-assisted rehabilitation: passive training and active training [10]. Passive training is employed during the initial phase of rehabilitation for patients, wherein they perform predetermined movements assisted by robots. On the other hand, active training is implemented in the later stages of rehabilitation, where patients exert force against the resistance provided by the robot to enhance their lower limb muscle strength [11]. However, a training method that combines elements of both passive and active training is gaining attention in the field of rehabilitation robots. This method, known as human-robot collaboration technology, aims to enhance the robot's comfort and prevent secondary injury to

* Corresponding author.

E-mail address: chenling@hebut.edu.cn (L. Chen).

the patient's body [12]. Therefore, patient-cooperative compliant control is crucial in rehabilitation robot control [13].

A compliance control strategy is a crucial consideration for ensuring efficiency, safety, and comfort during rehabilitation training [14–16]. Zhou et al. proposed a temporal compliance control strategy to enhance the safety and comfort of the robot during rehabilitation training. This strategy allows participants to adaptively modify the robot's motion trajectory based on the interaction force with the robot [17]. In [18], a robot joint with variable stiffness is designed to adjust the tension length of the elastic belt, enabling variable stiffness. The stiffness of the robot joints is adjusted in real-time to match the stiffness of the human arm. This allows for real-time compliant interaction in human-robot collaboration. Wu et al. [19] combined the interaction force and the surface electromyography signal of muscles to determine the human motion intention and conducted a human-cooperative robot-assisted training using an adaptive neural cooperative controller. Cheng et al. established a mapping relationship between the movement of the healthy side and the injured side of the lower limb of patients and applied a hierarchical control strategy to the mirror therapy of a rehabilitation robot. This approach improved the compliance and safety of the movement in the mirror therapy [20]. While all of the above studies have made significant progress in compliance control, the designed rehabilitation strategies have not explained the control effect of patients during passive rehabilitation training. To further enhance the efficiency and comfort of patient's rehabilitation training, this paper combines the two training mode, allowing the patient to engage in both passive rehabilitation training and patient-cooperative rehabilitation training.

Impedance and admittance control play a significant role in addressing the issue of interaction between humans and robots during rehabilitation training [21–23]. Chen et al. have proposed an estimation method for human-robot active torque to identify human motion intention. They also suggest a compliance control method based on impedance control to address the problem of muscle contraction disorder in patients during rehabilitation [24]. Zhang et al. have proposed a fuzzy impedance controller using the radial basis function and an outer loop impedance controller to handle uncertainty and improve the motion compliance of the human-robot coupling system [25]. Otten et al. [26] have utilized gravity compensation algorithms to reduce the burden on patients during the rehabilitation process, resulting in improved recovery levels, efficiency, and patient comfort. Admittance control has gained popularity in rehabilitation robots due to its advantageous compliance control capabilities in recent years [27]. Li et al. [28] investigated the effectiveness of the proposed adaptive admittance control algorithm in various environments, considering the influence of robots, humans, and the environment on the compliance of physical human-robot interaction. Zhang et al. [29] implemented a hierarchical adaptive patient cooperative control strategy in an ankle rehabilitation robot, utilizing an adaptive admittance controller at the higher level to adjust the motion trajectory based on the interaction force between the patient and the robot. Li et al. [30] identified the patient's motion intention through physical human-robot interaction and proposed a time-varying stiffness adaptive admittance control scheme to modify the motion state of the rehabilitation robot according to the patient's intention. Wu et al. [31] developed three movement modes for the rehabilitation robot and employed the proposed minimum intervention control strategy based on the admittance model to optimize the utilization of the patient's motor capacity for compliant movement.

The purpose of this paper is to develop a new adaptive patient-cooperative control strategy for a LLRR. This strategy aims to adjust the robotic assistance based on the patient's rehabilitation

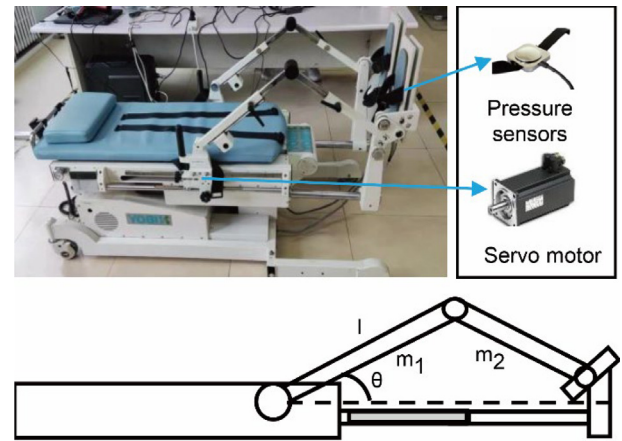


Fig. 1. Structure and model of LLRR.

level. In the early stages of rehabilitation training, a low compliance level is applied, and as the patient's muscle strength increases, an enhanced compliance level is implemented. This paper first establishes a dynamic model for the LLRR. Then, a hierarchical control system is designed, which includes a high-level adaptive admittance controller and a low-level position controller. Finally, experimental results demonstrate the effectiveness of the proposed control strategy.

2. Method

2.1. Dynamics of LLRR

The structure and model of the LLRR system are depicted in Fig. 1. Pressure sensors are employed to detect the contact force between the patient and the LLRR. The dynamic model is established based on the robot's structure. The dynamic model of the LLRR system with one leg is described as follows:

$$M(\theta)\ddot{\theta} + C(\theta, \dot{\theta})\dot{\theta} + G(\theta) = \tau + \tau_{hr} \quad (1)$$

In differential Eq. (1), θ , $\dot{\theta}$ and $\ddot{\theta}$ are the hip joint's angle, angular velocity, and angular acceleration of the rehabilitation robot, respectively. Besides, $M(\theta)$ is inertial matrix, $C(\theta, \dot{\theta})$ is the Coriolis and centrifugal matrix, $G(\theta)$ is robot's gravitational matrix, and τ is control torque applied to the joints, τ_{hr} is the interaction torque between the patient and robot.

The dynamic model of LLRR can be rewritten as a state space equation as follows:

$$\begin{cases} \dot{x}_1 = x_2 \\ \dot{x}_2 = f(x_1, x_2) + M^{-1}(x_1)u + M^{-1}(x_1)\tau_{hr} \end{cases} \quad (2)$$

where $x_1 = \theta$, $x_2 = \dot{\theta}$, $u = \tau$,

$$f(x_1, x_2) = -M^{-1}(x_1)(C(x_1, x_2) + G(x_1))$$

$$M(x_1) = (m_1 + m_2)l^2/3$$

$$C(x_1, x_2) = -2m_2l^2\sin x_1 \cos x_1$$

$$G(x_1) = ((m_1 + m_2)gl \cos x_1)/2$$

m_1 and m_2 are connecting rod mass of thigh and calf, l is the length of connecting rod of thigh and calf, g is the acceleration of gravity.

Assumption 1. Desired trajectory θ_d , desired trajectory velocity $\dot{\theta}_d$ and desired trajectory acceleration $\ddot{\theta}_d$ of hip joint are known, smooth, continuous, and bounded.

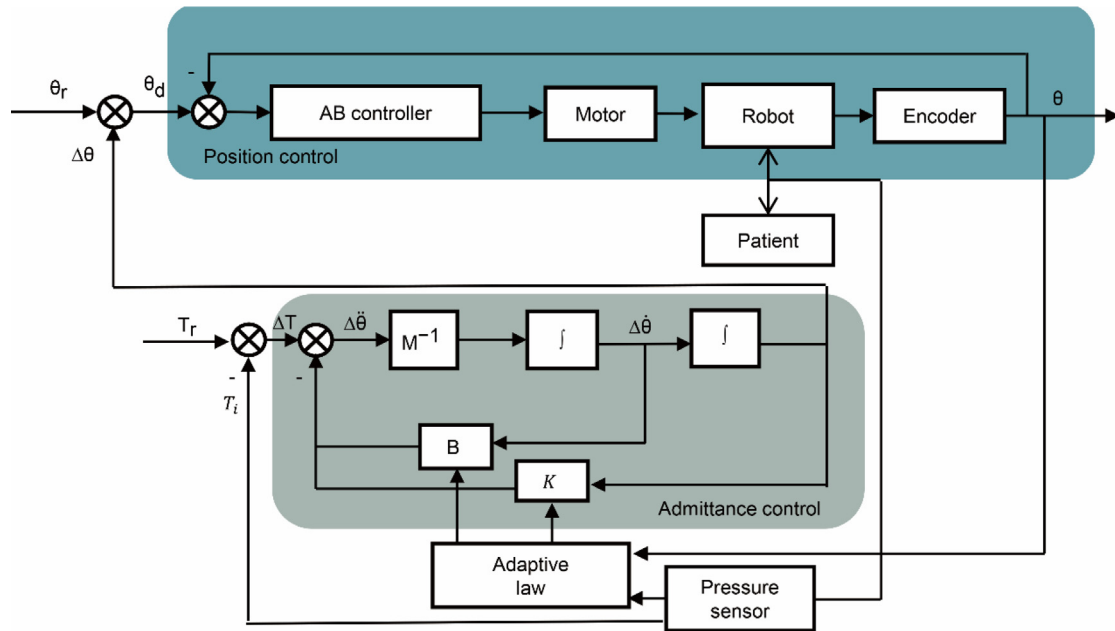


Fig. 2. Hierarchical control strategy implemented on the LLRR.

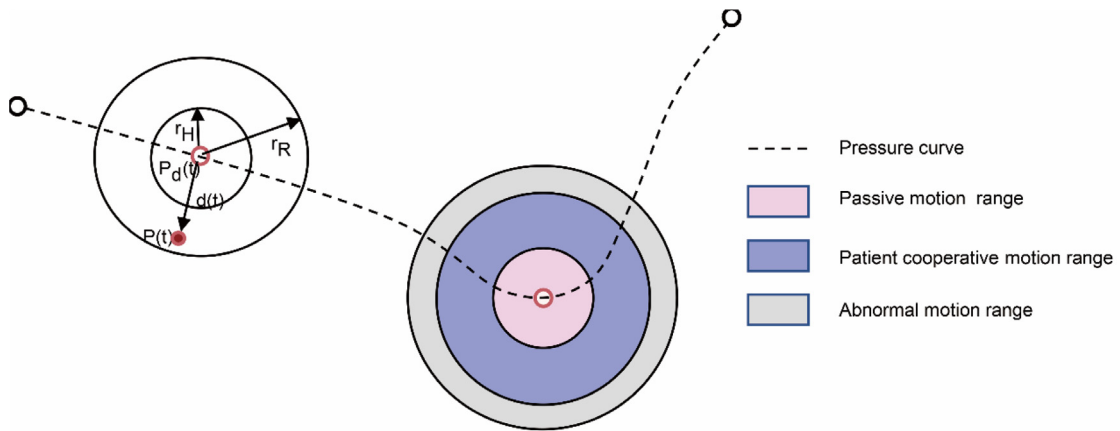


Fig. 3. Divide of three areas based on human-robot contact force.

Assumption 2. The thigh rod and calf rod of the LLRR have the same length. The mass of the thigh rod and calf rod is uniform and concentrated at the center of mass.

2.2. Adaptive patient-cooperative control

To enhance the motion compliance of the LLRR, a hierarchical control strategy is suggested. The strategy comprises of a high-level adaptive admittance controller and a low-level adaptive backstepping (AB) position controller. Fig. 2 illustrates the patient-cooperative control strategy for the LLRR. In the figure, θ_r , θ_d , and θ represent the hip joint reference trajectory, desired trajectory, and tracking trajectory, respectively. T_r denotes the interactive torque between the patient and robot during passive training, while T_i represents the torque actively applied by the patient.

During the rehabilitation training, the patient interacts with the robotic foot pedals. To ensure more accurate performance of different rehabilitation exercises, it is important to divide the range of human-robot interaction force into distinct divisions. The division method can be observed in Fig. 3.

In Fig. 3, the pressure curve represents the contact force between the patient and the robot during the patient's passive rehabilitation training. During this time, the patient does not exert active force on the robot. The pressure curve is divided into three different areas based on the force exerted by the patient on the rehabilitation robot. $P_d(t)$ represents the interaction force between the patient and the rehabilitation robot during passive rehabilitation training. $P(t)$ represents the force exerted by the patient on the rehabilitation robot. $d(t)$ represents the distance between $P_d(t)$ and $P(t)$. The range of $d(t)$ is from 0 to r_H , which represents the passive training range. In this range, LLRR performs passive rehabilitation training for patients using the low-level position controller. When the value of $d(t)$ is in the range $(r_H, r_R]$, it represents the patient-cooperative range. In this range, the high-level admittance controller is activated to adjust the motion trajectory. $(P(t) - r_H)$ represents the active force applied to the robot to adjust the desired trajectory until $P(t)$ returns to the passive training range. The variable $d(t) \in (r_H, +\infty)$ indicates the abnormal motion range, which signifies that the patient is exhibiting abnormal movement. It is crucial for the patient's safety to halt rehabilitation training in such cases. Therefore, this paper proposes a patient-cooperative control strategy that can

adapt the training mode based on the human–robot contact force. The primary focus of this study will be on the passive motion range and the patient cooperative motion range.

2.2.1. Joint-space position controller

At the beginning of therapy, the patient exhibits relatively weak muscle strength. To gradually restore the patient's movement ability, the LLRR utilizes passive training. The low-level position controller, which comprises an adaptive backstepping controller commonly employed in nonlinear systems, is responsible for tracking the trajectory. This paper applies an adaptive backstepping method to the LLRR, allowing it to adapt to the uncertain parameters τ_{hr} and achieve trajectory tracking. The adaptive rate of the human–interaction force is determined as follows:

$$\dot{\hat{\tau}}_{hr} = (x_2 - \dot{x}_d + x_1 - x_d)M^{-1}(x_1) \quad (3)$$

where $\hat{\tau}_{hr}$ is the approximation value of τ_{hr} , Adaptive backstepping control rate u is as follows:

$$u = - \int_0^t (x_2 - \dot{x}_d + x_1 - x_d) M^{-1}(x_1) dt + M(x_1)(\ddot{x}_d - 2\dot{x}_2 + 2\dot{x}_d - 2x_1 + 2x_d - f(x_1, x_2)) \quad (4)$$

where $\ddot{x}_d = \ddot{\theta}_d$, $\dot{x}_d = \dot{\theta}_d$ and $x_d = \theta_d$ are hip joint desired trajectory acceleration, desired trajectory velocity and desired trajectory, respectively.

2.2.2. Task-space admittance controller

Pure position control cannot be used for patient cooperative rehabilitation training due to the consideration of human–robot interaction force as disturbances. This paper proposes the use of a high-level adaptive admittance control to adjust the trajectory. Admittance control adjusts the output displacement based on the input force. The admittance control model is represented by Eq. (5).

$$T_r(t) - T_i(t) = M\Delta\ddot{\theta}(t) + B\Delta\dot{\theta}(t) + K\Delta\theta(t) \quad (5)$$

M , B , and K represent the inertia, damping, and stiffness coefficients, respectively. The admittance model can be used to adjust the robot's motion trajectory based on the interaction force between the human and the robot. When the interaction force disappears, the robot's motion trajectory returns to the predefined reference trajectory. However, it is important to note that different patients may require different levels of assistance during rehabilitation training. Therefore, it is necessary for the robot to have variable compliance based on the rehabilitation level of each individual patient.

2.2.3. Adaptation law

To enhance compliance in rehabilitation training, it is crucial for the robot to provide adjustable assistive measures. This study proposes an adaptation law to modify the admittance parameters. The parameters B and K are adjusted using Eqs. (6) and (7), where B_0 and K_0 represent the base values. The coefficients a_j and b_j ($j = 1, 2, 3$) are used to modify the damping and stiffness of the robot's admittance model. Additionally, B_{1j} and K_{1j} ($j = 1, 2$) represent the upper and lower thresholds for damping and stiffness. The interaction force T between the human and robot is measured using a plantar pressure sensor and a data acquisition card.

Set thresholds for the adaptive rate of damping and stiffness parameters to ensure the stability of the control system. From Eqs. (6) and (7), B and K can be adjusted based on the angle and force. As the robot's angular and interaction force increase, B and

K decrease. This ensures the safety and comfort of patients when the human–robot interaction force increases.

$$B = \begin{cases} B_{11}, B < B_{11} \\ B_0 \frac{1}{a_1 e^{|a_2 \theta|}} |a_3/T|, B_{11} < B < B_{12} \\ B_{12}, B > B_{12} \end{cases} \quad (6)$$

$$K = \begin{cases} K_{11}, K < K_{11} \\ K_0 \frac{1}{b_1 e^{|b_2 \theta|}} |b_3/T|, K_{11} < K < K_{12} \\ K_{12}, K > K_{12} \end{cases} \quad (7)$$

2.2.4. Evaluation method

DSJ and NRMSD are quantitative evaluation indicators of different trajectory planners. The DSJ and the NRMSD is described as follows:

$$DSJ = \int_{t_a}^{t_b} \ddot{\theta}(t)^2 dt \frac{(t_b - t_a)^5}{A^2} \quad (8)$$

$$NRMSD = \frac{\sqrt{\frac{\sum_{j=1}^n e^2(t_j)}{n}}}{\max(q_d) - \min(q_d)} \quad (9)$$

where A is the maximum amplitude of the trajectory. The time when the trajectory starts and ends can be denoted as t_a and t_b , respectively. Here $j = 1, 2, \dots, n$ represents the sample number, and $e(t_j)$ represents the error between the desired trajectory and tracking trajectory at the time t_j . Additionally, $\max(q_d)$ and $\min(q_d)$ represent the maximum and minimum position of the trajectory, respectively. It is worth noting that a smaller DSJ value and NRMSD value indicate a more compliant movement and a higher tracking accuracy.

3. Simulation and experiment

3.1. Simulation results

In this study, we simulated and implemented the variable admittance (VA) and fixed admittance (FA) control strategies on a robot using MATLAB (2019b). By adjusting the admittance parameters, we were able to achieve different levels of trajectory compliance. The control methods were selected based on the forces applied to the robot, allowing for varying degrees of motion compliance.

3.1.1. Simulation of FA and VA

To investigate the properties of FA and VA, simulation experiments are conducted using MATLAB (2019b). The interaction force is denoted as $f(t)$ and can be formulated as follows:

$$f(t) = \begin{cases} 1, 2 \leq t \leq 5 \\ 0, \text{otherwise} \end{cases} \quad (10)$$

The reference trajectory θ_r is set as zero. The simulation results of FA and VA are shown in Fig. 4. From Fig. 4(a), (b), and (c), it can be observed that the inertia, damping, and stiffness parameters have different effects on the amplitude and convergence time of the desired trajectory. It is important to note that an inappropriate inertia parameter can lead to oscillations in the desired trajectory. Additionally, in Fig. 4(d) and (e), it is evident that the desired acceleration, desired velocity, and desired trajectory generated by VA are smaller than those generated by FA during the transitioning stage (from contact to non-contact).

3.1.2. Simulation of control strategy

Simulations of the hierarchical control strategy is carried in MATLAB. The interactive force between patient and robot $f(t)$ is defined as follows:

$$f(t) = \begin{cases} 10, (2 \leq t \leq 3) \cup (7 \leq t \leq 8) \\ 0, \text{otherwise} \end{cases} \quad (11)$$

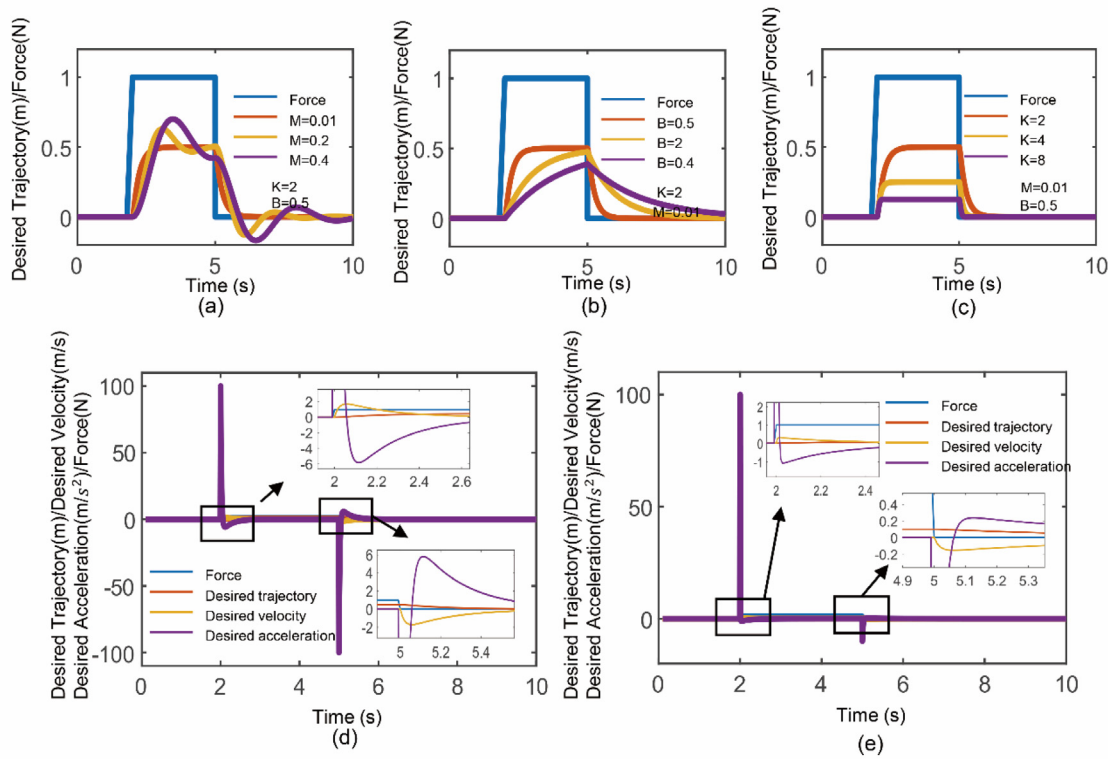


Fig. 4. Simulation results for different trajectory planners. (a), (b) and (c) are simulated with different model parameters. (d) are the simulated results of FA. (e) are the simulated results of VA proposed in this study.

Table 1
Structural parameters of LLRR.

Symbol	Description	Thigh ($i = 1$)	Calf ($i = 1$)
m_i (kg)	The mass of LLRR	2.46	3.14
l_i (m)	The length of LLRR	0.51	0.51
d_i (m)	The distance from center of mass to joint	0.43	0.18
I_i (kg·m ²)	The inertias of LLRR	0.52	0.21

Table 2
Parameters of adaptive admittance control.

Symbol	Description	Value	Units
M	Inertia	0.01	N·m/(rad·s ²)
B_0	Damping base values	0.5	N·m/(rad·s)
K_0	Stiffness base values	2.0	N·m/rad
a_1, b_1	Parameter of Damping and Stiffness	1.2	-
a_2, b_2	Parameter of Damping and Stiffness	0.2	-
a_3, b_3	Parameter of Damping and Stiffness	1.5	-
B_{11}, K_{11}	Upper thresholds of Damping and Stiffness	5	N·m/(rad·s), N·m/rad
B_{12}, K_{12}	Lower thresholds of Damping and Stiffness	20	N·m/(rad·s), N·m/rad

The kinetic equation of the LLRR has been derived in Eqs. (1). The relevant structural parameters and parameters of adaptive admittance control are presented in Tables 1 and 2. The adaptive backstepping position controller with FA and VA are referred to as AB-FA and AB-VA, respectively. A kinematic analysis of the LLRR was conducted to convert the hip joint angle into the displacement of the robot's joint ends.

As depicted in Fig. 5, the trajectory planners have the ability to adjust the reference trajectory to the desired trajectory when there is a human-robot interaction force. Once the human-robot interaction force disappears, the desired trajectory gradually converges back to the reference trajectory. Notably, the convergence time of AB-VA is shorter than that of AB-FA. The quantitative evaluation results of AB-VA and AB-FA are presented in Table 3. In

Table 3
Results of simulation.

Control strategy	DSJ of desired trajectory	DSJ of tracking trajectory	NRMSD (%)
AB-VA	2.44560×10^7	2.3634×10^7	0.012
AB-FA	2.5253×10^7	2.4609×10^7	0.009

terms of compliance performance, the DSJ value of the trajectory generated by AB-VA is smaller than that of AB-FA. This outcome demonstrates that the VA can enhance robot compliance. Furthermore, the NRMSD values of AB-VA and AB-FA are similar, indicating that the trajectory tracking effects of the two methods are comparable.

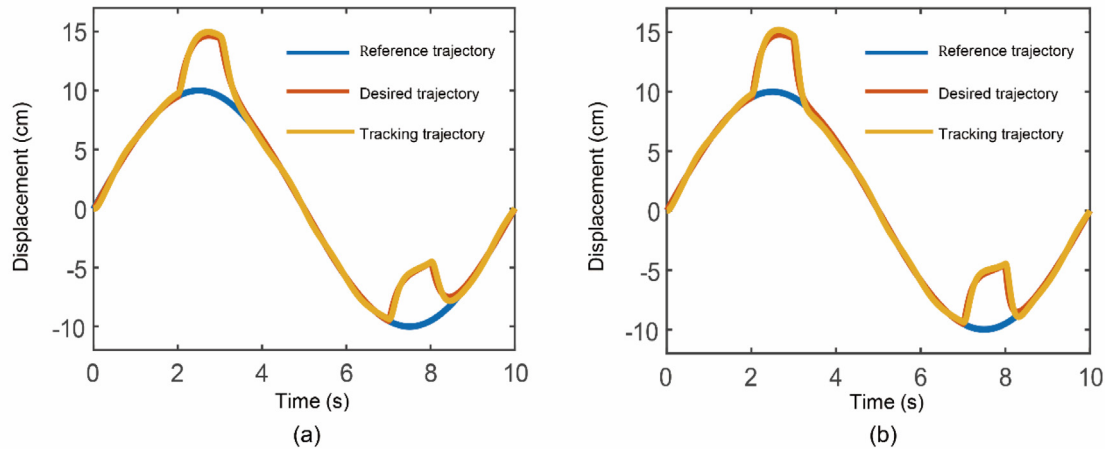


Fig. 5. Simulation results of different control strategy. (a) the results of AB-VA. (b) the results of AB-FA.

3.2. Experimental results

In this section, the proposed control strategy is applied to conduct experiments on four healthy subjects, and the experimental results are presented. All four individuals voluntarily agreed to participate in the experiment after obtaining ethical approval from the Ethics Committee of Hebei University of Technology. Applying the hierarchical compliance control strategy to lower limb rehabilitation robots, the servo motor power of the robot is 0.75kw, the encoder resolution is 20 bits, and the working voltage is AC 220 V.

To evaluate the effectiveness of the control strategy, we conducted a patient-cooperative control experiment on the LLRR. During passive rehabilitation training, we collected the human-robot contact force T_r to determine the appropriate upper limit r_H . The contact force of the subject during a passive rehabilitation training cycle, which includes contraction and extension, is depicted in Fig. 6. The scaled force was derived from the raw data. As shown in Fig. 6, the human-robot interaction force reaches its maximum when the patient completes the contraction movement. Subsequently, the force gradually decreases during the extension movement. Based on the findings from Fig. 6, we set the upper limit of the passive rehabilitation training range r_H to 0.5. This means that if the interaction force between the human and robot exceeds 0.5, the motion trajectory will be adjusted accordingly.

During the experimental process of patient cooperation, the subject was instructed to apply active torque to simulate an unknown dynamic contact environment. When the active force applied by the patient falls within the patient's cooperative range of motion, as shown in Fig. 3, the LLRR system enters the patient cooperation training mode. The robot then adjusts its motion trajectory until the human-robot interaction force returns to the passive motion range.

The results of a patient-robot cooperation experiment using fixed admittance parameters are depicted in Fig. 7. Fig. 7(b) illustrates the contact force between the subject and the robot. A high level indicates that the subject actively exerts force on the robot, while a low level implies that the robot is in passive rehabilitation training mode. When the subject's active force falls within the range of patient cooperative movement, the robot adjusts the reference trajectory to the desired trajectory based on the magnitude of the active force, and then tracks the desired trajectory. Once the active force between the subject and the robot returns to the passive training range, the desired trajectory gradually converges back to the reference trajectory, and the

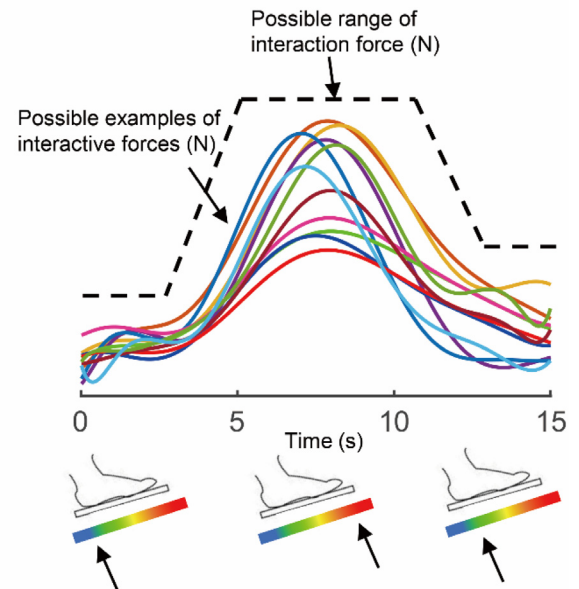


Fig. 6. Human-robot contact force during the passive rehabilitation training.

robot enters passive training mode. In Fig. 7(a) and Fig. 7(b), during the time intervals of 1.17–3.12 s, 4.68–8.58 s, and 9.88–12.22 s, the subject exerts an active force on the robot, causing the desired trajectory to deviate from the reference trajectory in accordance with the interaction force. At other times, the desired trajectory gradually converges back to the reference trajectory.

The experiment on patient-robot cooperation utilized variable admittance parameters with B and K , which were adjusted based on Eqs. (6) and (7). The results are presented in Fig. 8. The images in Fig. 8 convey the same physical meaning as Fig. 7. In Fig. 8(a) and Fig. 8(b), the subject exerted an active force on the robot during the time intervals of 0.26–2.86 s, 4.42–8.19 s, and 10.01–11.7 s. The desired trajectory deviated from the reference trajectory in accordance with the interaction force.

The quantitative evaluation of the two methods is presented in Fig. 9. It can be observed from the figure that the DSJ of the desired trajectory generated by AB-VA is 7.18% lower than that created by AB-FA. Similarly, the DSJ of the tracking trajectory generated by AB-VA is 76.45% lower than that created by AB-FA. Additionally, the NRMSD of the tracking trajectory generated

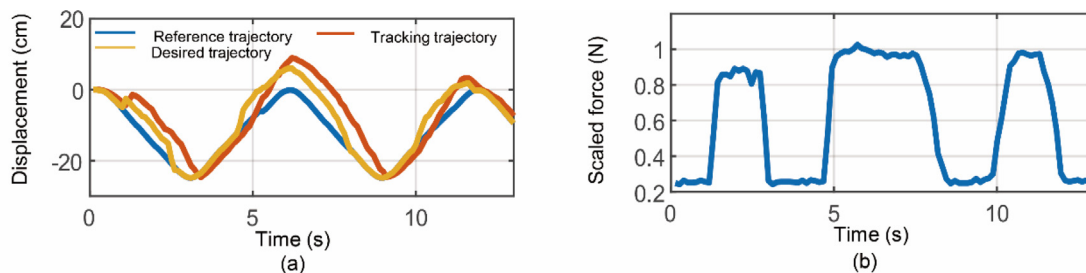


Fig. 7. Experimental results of the patient-cooperative control with FA. (a) trajectory tracking result of AB-FA. (b) human-robot interaction force.

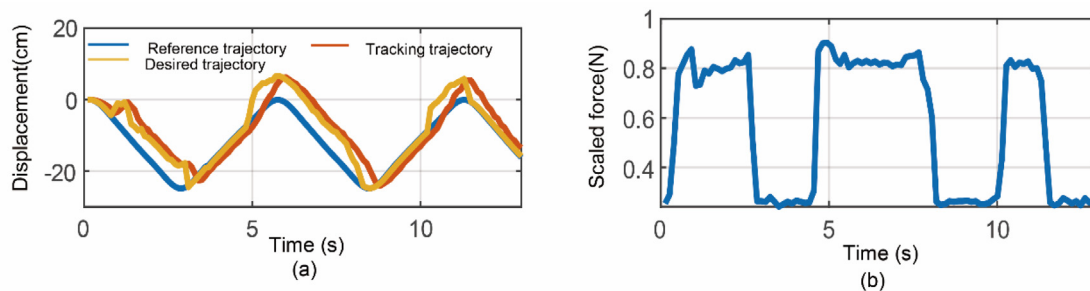


Fig. 8. Experimental results of the patient-cooperative control with VA. (a) trajectory tracking result of AB-VA. (b) human-robot interaction force.

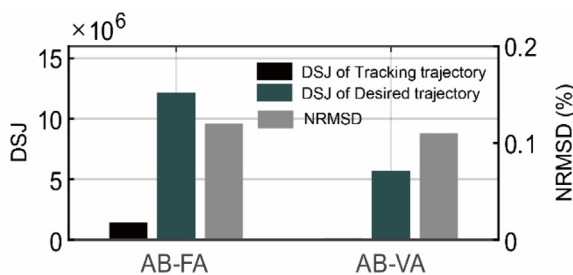


Fig. 9. Quantitative evaluation of AB-VA and AB-FA.

by AB-VA is 15.38% lower than that created by AB-FA. These quantitative analysis results demonstrate that the control strategy proposed in this paper effectively enhances the compliance of the LLRR.

4. Conclusions

This paper proposes a hierarchical control strategy to enhance robot motion compliance. The strategy consists of a low-level position controller and a high-level admittance controller. The interaction force between the patient and the robot is divided into different areas, and different control modes are applied based on the contact force. In the case of low interaction force, the low-level position controller is used to passively track the robot's motion trajectory during training. When the interaction force is within the defined range of patient cooperative motion, the high-level admittance controller is activated. This controller adjusts the robot's motion trajectory based on the active force exerted by the patient. Simulation and experimental results using fixed and adaptive admittance parameters demonstrate that the adaptive admittance control yields smaller NRMDS and DSJ values.

The smoothness of motion control is crucial for lower limb rehabilitation robots as it promotes human-robot interaction and enhances the effectiveness of rehabilitation training. However, the control system's stability can be compromised by the unknown dynamic contact environment, resulting in a significant

reduction in motion compliance. In comparison to AB-FA, AB-VA offers greater motion compliance through human-robot interaction forces, particularly in unstable contact environments. AB-VA allows patients to have greater freedom of movement, enhancing their comfort during active rehabilitation training and encouraging active participation.

The proposed techniques aim to enhance the comfort and safety of robot-assisted rehabilitation training in three aspects. Firstly, a hierarchical control strategy is suggested, which combines passive and cooperative rehabilitation training to cater to a wider range of lower limb dysfunction patients at different stages. Additionally, the plantar pressure is divided into different regions, allowing patients to adjust their rehabilitation training mode in real-time based on their recovery situation, thereby achieving personalized rehabilitation. Lastly, adaptive admittance control is proposed, limiting the range of damping and stiffness parameters to improve patient training comfort and ensure training process safety.

When dividing the range of interaction force between humans and robots, fixed upper and lower thresholds are used to define different areas. To enhance the robot's adaptability to different patients, future work will involve establishing a model of the interaction force between human body parameters and the robot during passive rehabilitation training. This model will allow individual patients to adjust the upper and lower thresholds of each area based on their own weight, thereby improving the robot's adaptability to a variety of patients.

Declaration of competing interest

The authors declare that they have no known competing financial interests or personal relationships that could have appeared to influence the work reported in this paper.

Acknowledgments

This work was supported by grants from the S&T Program of Hebei (22372001D), the Natural Science Foundation of Hebei Province, China (F2021202021), and the National Key R&D Program of China (2019YFB1312500).

Ethics approval

This work was approved by the Biomedical Ethics Committee of Hebei University of Technology (NO. HEBUTHMEC2022005).

Appendix A. Supplementary data

Supplementary material related to this article can be found online at <https://doi.org/10.1016/j.birob.2024.100155>.

References

- [1] Y. Zhang, X. Liu, X. Qiao, et al., Characteristics and emerging trends in research on rehabilitation robots from 2001 to 2020: bibliometric study, *J. Med. Internet Res.* 25 (2023) 42901.
- [2] Y.M. Khalid, D. Gouwanda, S. Parasuraman, A review on the mechanical design elements of ankle rehabilitation robot, *P. I. Mech. Eng. H.* 229 (6) (2015) 452–463.
- [3] H.M. Qassim, WZ.Wan. Hasan, A review on upper limb rehabilitation robots, *Appl. Sci.* 10 (19) (2020) 6976.
- [4] S. Bhardwaj, A.A. Khan, M. Muzammil, Lower limb rehabilitation robotics: the current understanding and technology, *Technol. Health Care* 69 (2021) 775–793.
- [5] S. Hussain, S. Xie, P.K. Jamwal, Robust nonlinear control of an intrinsically compliant robotic gait training orthosis, *IEEE Trans. Syst. Man Cybern.: Syst.* 43 (3) (2013) 655–665.
- [6] L.M. Weber, J. Stein, The use of robots in stroke rehabilitation: A narrative review, *Technol. Health Care* 43 (2018) 99–110.
- [7] P.K. Jamwal, S. Xie, S. Hussain, et al., An adaptive wearable parallel robot for the treatment of ankle injuries, *IEEE/ASME Trans. Mechatron.* 19 (1) (2014) 64–75.
- [8] Y. Peng, Y. Sakai, K. Nakagawa, et al., Funabot-suit: A bio-inspired and McKibben muscle-actuated suit for natural kinesthetic perception, *Biomimetic Intell. Rob.* 3 (4) (2023) 100127.
- [9] F. Dong, H. Li, Y. Feng, Mechanism design and performance analysis of a sitting/lying lower limb rehabilitation robot, *Machines* 10 (8) (2022) 674.
- [10] P. Poli, G. Morone, G. Rosati, et al., Robotic technologies and rehabilitation: new tools for stroke patients' therapy, *Biomed. Res. Int.* 2013 (2013) 153872.
- [11] L. Zhang, S. Guo, Q. Sun, An assist-as-needed controller for passive, assistant, active, and resistive robot-aided rehabilitation training of the upper extremity, *Appl. Sci.* 11 (1) (2021) 340.
- [12] G. Masengo, X. Zhang, R. Dong, et al., Lower limb exoskeleton robot and its cooperative control: A review, trends, and challenges for future research, *Front. Neurobot.* 16 (2023) 913748.
- [13] H. Yu, S. Huang, G. Chen, et al., Human–robot interaction control of rehabilitation robots with series elastic actuators, *IEEE Trans. Rob.* 31 (5) (2015) 1089–1100.
- [14] D. Shi, W. Zhang, W. Zhang, et al., A review on lower limb rehabilitation exoskeleton robots, *Chin. J. Mech. Eng.* 32 (1) (2019) 1–11.
- [15] T. Eiammanussakul, V. Sangveraphunsiri, A lower limb rehabilitation robot in sitting position with a review of training activities, *J. Healthc. Eng.* 2018 (2018) 1927807.
- [16] J.K. Mohanta, S. Mohan, P. Deepasundar, et al., Development and control of a new sitting-type lower limb rehabilitation robot, *Comput. Electr. Eng.* 67 (2018) 330–347.
- [17] J. Zhou, H. Peng, S. Su, et al., Spatiotemporal compliance control for a wearable lower limb rehabilitation robot, *IEEE Trans. Biomed. Eng.* 70 (6) (2022) 1858–1868.
- [18] X. Zhang, L. Huang, H. Niu, Structural design and stiffness matching control of bionic variable stiffness joint for human–robot collaboration, *Biomimetic Intell. Rob.* 3 (1) (2023) 100084.
- [19] Q. Wu, Y. Chen, Development of an intention-based adaptive neural cooperative control strategy for upper-limb robotic rehabilitation, *IEEE Rob. Autom. Lett.* 6 (2) (2021) 335–342.
- [20] G. Cheng, L. Xu, Compliance control of a lower limb rehabilitation robot in mirror therapy, in: 7th International Conference on Mechatronics and Robotics Engineering, 2021, pp. 77–82.
- [21] X. Zhang, Z. Yue, J. Wang, Robotics in lower-limb rehabilitation after stroke, *Behav. Neurol.* (2017) 3731802.
- [22] J. Wu, J. Gao, R. Song, et al., The design and control of a 3DOF lower limb rehabilitation robot, *Mechatronics* 33 (2016) 13–22.
- [23] S. Bhardwaj, A.A. Khan, M. Muzammil, Lower limb rehabilitation robotics: the current understanding and technology, *Work* 69 (3) (2021) 775–793.
- [24] J. Chen, Y. Huang, X. Guo, et al., Parameter identification and adaptive compliant control of rehabilitation exoskeleton based on multiple sensors, *Measurement* 159 (2020) 107765.
- [25] P. Zhang, J. Zhang, A. Elabbagh, Fuzzy radial-based impedance controller design for lower limb exoskeleton robot, *Robotica* 41 (1) (2023) 326–345.
- [26] A. Otten, C. Voort, A. Stienen, et al., Limpact: A hydraulically powered self-aligning upper limb exoskeleton, *IEEE/ASME Trans. Mechatron.* 20 (5) (2015) 2285–2298.
- [27] H.T. Tran, H. Cheng, R. Huang, et al., Evaluation of a fuzzy-based impedance control strategy on a powered lower exoskeleton, *Int. J. Social Rob.* 8 (1) (2016) 103–123.
- [28] H.Y. Li, I. Paranawithana, L. Yang, et al., Stable and compliant motion of physical human–robot interaction coupled with a moving environment using variable admittance and adaptive control, *IEEE Rob., Autom. Lett.* 3 (3) (2018) 2493–2500.
- [29] M. Zhang, S. Xie, X. Li, et al., Adaptive patient-cooperative control of a compliant ankle rehabilitation robot (CARR) with enhanced training safety, *IEEE Trans. Ind. Electron.* 65 (2) (2018) 1398–1407.
- [30] B. Huang, Z. Li, C. Yang, et al., Physical human–robot interaction of a robotic exoskeleton by admittance control, *IEEE Trans. Ind. Electron.* 65 (12) (2018) 9614–9624.
- [31] Q. Wu, X. Wang, B. Chen, et al., Development of a minimal-intervention-based admittance control strategy for upper extremity rehabilitation exoskeleton, *IEEE Trans. Syst. Man Cybern.: Syst.* 48 (6) (2018) 1005–1016.